

# A Simplified Transient Flow Model for Riser Gas Handling in Non-Aqueous Muds with Time-Dependent Desorption Considerations

Nnamdi Nwaka, Yuanhang Chen, Otto Santos and Wesley Williams, Louisiana State University

Copyright 2019, AADE

This paper was prepared for presentation at the 2019 AADE National Technical Conference and Exhibition held at the Hilton Denver City Center, Denver, Colorado, April 9-10, 2019. This conference is sponsored by the American Association of Drilling Engineers. The information presented in this paper does not reflect any position, claim or endorsement made or implied by the American Association of Drilling Engineers, their officers or members. Questions concerning the content of this paper should be directed to the individual(s) listed as author(s) of this work.

## Abstract

Consideration of the degassing of gas influx from oil-based muds (OBM) is of significance while predicting the behavior of an influx during migration and circulation out of a marine riser. This paper presents a simplified transient flow model to predict riser gas behavior which adopts a kinetic sub-model recently developed to account for a time-dependent desorption of gas influx from OBM during migration and circulation.

The capability of this simplified model to realistically describe gas-in-riser events is examined by comparing simulation results to those obtained from our in-house simulators based on drift flux model. The depths of maximum void fraction and pressures at the blowout preventer obtained from both analyses are very comparable.

Prediction of the severity of unloading is seen to be very sensitive to consideration of degassing as a time dependent process. The severity of unloading and depth of the point of initiation of rapid is overestimated when a time dependent desorption is not considered. Sensitivity analyses are conducted to understand the dependence of the unloading behavior on the specific rate of degassing. Unloading is more severe for increasing values of desorption coefficient with significant differences in the final gas flow rates and pressures. This new model can accurately simulate gas-in-riser events with much less computational time making it more suitable for real-time riser gas management that can be extended to managed pressure drilling.

## Introduction

Gas in riser events present a complex problem to the offshore drilling industry. Gas in riser events will occur after a well has taken in a gas kick and this kick gets into the riser. This becomes especially important because it is complementary to controlling the gas kick in the already shut-in well. During the migration of the free gas in the riser (by buoyancy or circulation), a point exists in the riser mentioned in the literature<sup>9</sup> as the “riser equilibrium point”. At the riser equilibrium point, the gas velocities begin to increase dramatically and what is known as “rapid riser unloading”

begins until all the free gas have left the riser. Thus, whether the gas is circulated out or allowed to migrate, the riser equilibrium point must be met.

The rapid unloading of this gas is of serious concern to well control because of the threat this uncontrolled flow of gas will pose to personnel, environment and the rig itself. The riser could be subject to collapse pressures when this rapid unloading occurs. Because riser gas will expand and unload rapidly, controlled and timely circulation becomes key to mitigating these events. Pressure control devices and diverters serve as safety devices in riser unloading. It is necessary, however, to understand the mechanism of occurrence to facilitate accurate prediction and justify the use of prescribed safety devices.

It is not uncommon to neglect the effect of mass transfer in two-phase flow modeling and assume a water base mud (WBM) scenario. However, in oil-based muds (OBMs), influx dissolves in the mud. In high-temperature, high-pressure situations, gas can get dissolved infinitely in the diesel<sup>2</sup>. This gas will begin to breakout of solution when the pressure reduces. Now, in a marine riser (except when backpressure is increasingly applied within installation limits) there is continuous reduction in fluid pressure as the influx mud mixture moves upwards. This will provide more free gas for expansion and a more dramatic unloading.

In this paper, we formulate a simplified model to simulate influx being circulated out of a marine riser up to the point of riser equilibrium. This model calculates the pressure transients, the depth of riser equilibrium, the gas velocities and flowrates during circulation and rapid unloading, the pressure at the BOP and several other parameters. We also quantify the degassing of mud as a time-dependent process instead of an instantaneous process because, in reality, the degassing of mud takes some amount of time when conditions are met. Contribution to free gas does not happen instantaneously. We factor this in and see the effect on results. A time-dependent kinetic sub-model developed earlier<sup>4</sup> is used to calculate the mass transfer rate. This new model seeks to best represent real life occurrences of gas in riser events.

## Mathematical Model

### Two Phase Model

If the riser-booster line system is considered a U-tube, the pressure at any point in the riser annulus will be determined as a sum of the hydrostatic and hydrodynamic pressures calculated from that point to the surface.

At the point we have the top of the contaminated mud section, that pressure will be

$$p_G = p_{G0} = p_c + \rho_L g h_G + \frac{2f v_G^2 \rho_L h_G}{D_o - D_i} \quad (1)$$

And within the contaminated mud section, the instantaneous pressure is obtained by

$$\frac{\partial p_G}{\partial x} = g \rho_M + \frac{2f v_M^2 \rho_M}{D_o - D_i} \quad (2)$$

The friction factor  $f$ , is a function of the two-phase Reynolds number.

For turbulent flow ( $Re_{tp} \geq 3000$ ), the  $f$  is defined by<sup>1</sup>

$$f = 0.052 (Re_{tp})^{-0.19} \quad (3)$$

For laminar flow ( $Re_{tp} \leq 2000$ ), the  $f$  is defined by<sup>1</sup>

$$f = \frac{24}{Re_{tp}} \quad (4)$$

To obtain  $f$  within the range  $2000 \leq Re_{tp} \leq 3000$ , we use interpolation.

From (2),

$$\rho_M = E_G \rho_G + E_L \rho_L \quad (5)$$

We obtain a volume of free gas by

$$V_G = m_G / \rho_G(p, T) \quad (6)$$

The temperature is calculated using a known temperature profile, although this assumption has been obviated by some authors<sup>10,11</sup>. A compositional EOS is used instead of correlational in determining fluid properties.

The velocity of the top of the gas bubble is obtained as

$$v_G = C_m + \frac{1}{AE_G} \frac{\partial V_G}{\partial t} \quad (7)$$

$C_m$  is considered the velocity at the tail of the gas section and it is related to position by

$$\frac{\partial h_m}{\partial t} = -C_m \quad (8)$$

But  $C_m$  is obtained by an analytical slip law as

$$C_m = C_0 v_M + v_{Gr} \quad (9)$$

And because we consider bubbly flow (because field tests have shown that gas-bubble formation in risers is governed through dispersion rather than slug-type behavior patterns<sup>7</sup>) we use the Hibiki and Ishii<sup>3</sup> correlation for bubbly flow to obtain the slip parameters thus,

$$C_0 = 1.2 - 0.2 \sqrt{\rho_G / \rho_L} (1 - \exp(-18E_G)) \quad (10)$$

$$v_{Gr} = 1.41 (g \sigma \Delta \rho / \rho_L^2)^{0.25} (1 - E_G)^{1.75} \quad (11)$$

The void fraction will however be affected by the amount of free gas degassed which will be based also on the pressure drop during circulation. This makes the modeling more complicated than no-mass transfer assumption.

The mixture velocity is obtained thus:

$$v_M = \frac{Q_0}{A} \quad (12)$$

The instantaneous position of the point with the highest void fraction is obtained as

$$h_G = h_m - \frac{V_G}{AE_G} \quad (13)$$

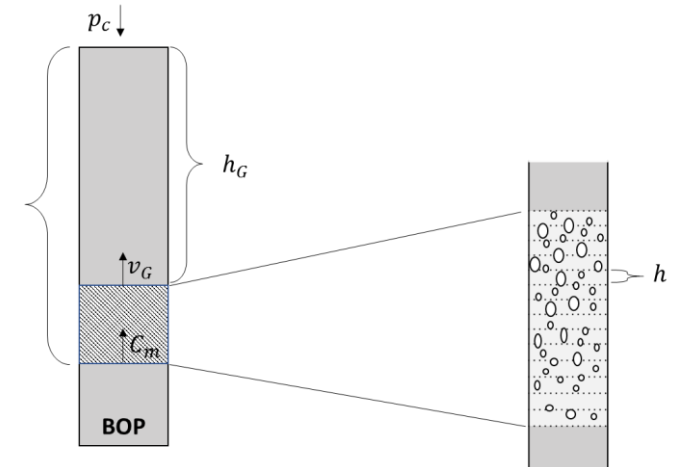


Figure 1: Discretization of the contaminated mud section containing free gas and dissolved gas

### Gas and Liquid Viscosity

The liquid viscosity is assumed constant throughout the pipe and because the gas viscosity is an important parameter in the determination of the frictional backpressure, the gas viscosity is obtained by the following equations as proposed by Lee et al.<sup>14</sup>.

$$\mu_g = 10^{-7} K \exp \left[ X \left( \frac{\rho_g}{1000} \right)^Y \right] \quad (14)$$

$$K = \frac{(19.919 + 36M_g)T^{1.5}}{64.506 + 5846.222M_g + T} \quad (15)$$

$$X = 0.01 \left( 350 + \frac{30432.1}{T} + 1000M_g \right) \quad (16)$$

$$Y = 0.2(12 - X) \quad (17)$$

### Desorption Model

Most two-phase flow simulations operate under the assumption of no mass transfer. However, this is not so since for two-phase flow with similar composition, at the right conditions, there will be transfer from one phase to the other. Often in drilling, gas influx is dissolved in the liquid phase under specified conditions and when these conditions are forgone, a reverse transfer will begin to occur. In circulating mud containing dissolved gas out of the riser, gas will come out of solution as the gas-mud mixture moves up the riser. We assume that the NAM is saturated with dissolved gas when it is at the bottom of the riser, with some presence of free gas. The manner of release of this free gas from solution is investigated. Calculations are made under the assumption that the mud does not degas instantaneously but time dependent. To quantify this process, we adopt the kinetic sub-model formulated by Linga et al.<sup>4</sup> where the rate of desorption is a function of the amount of dissolved gas. In this model, an experimentally determined mass transfer coefficient is used. This coefficient depends primarily on the composition of the two phases<sup>4,12</sup>.

The rate of change of gas loading capacity in mud is given as

$$\frac{\partial R_s}{\partial t} = K_d(R_{smax} - R_s), \quad R_s \geq R_{smax} \quad (18)$$

The mass transfer from this desorption process has a significant effect on the volume of free gas as it migrates upwards and thus affects calculations. Degassing causes changes in the void fractions and the migration velocities, in addition to the dependence of these parameters to pressure. The void fraction increases more as the influx moves upward. Since (18) is a first order ODE, the solution is obtained as

$$R_{s_{n+1}} = R_{s_{max_n}} + (R_{s_n} - R_{s_{max_n}}) e^{-K_d t} \quad (19)$$

The  $R_{s_{max}}$  at every step is obtained using the O'Bryan et al.<sup>5</sup> relation (assuming only diesel for simplicity) given as:

$$R_{s_{max}} = \left( \frac{p}{aT^b} \right)^c \quad (20)$$

Where  $a$ ,  $b$  and  $c$  are defined for the diesel gas mixture and the temperature.

To obtain the initial values, the initial top of contaminated mud section and the initial void fraction (assumed uniform along the column) are determined in a single iteration. (21) is optimized at every iteration step to obtain a new  $E_{G0}$ . **Fig 2.** shows a flowchart to obtain initial values.

$$1.53 \left[ \frac{g(\rho_L - \rho_G)\sigma}{\rho_L^2} \right]^{0.25} (1 - E_G)^{0.5} \sin\theta = \frac{v_{SG}}{E_G} - 1.2v_M \quad (21)$$

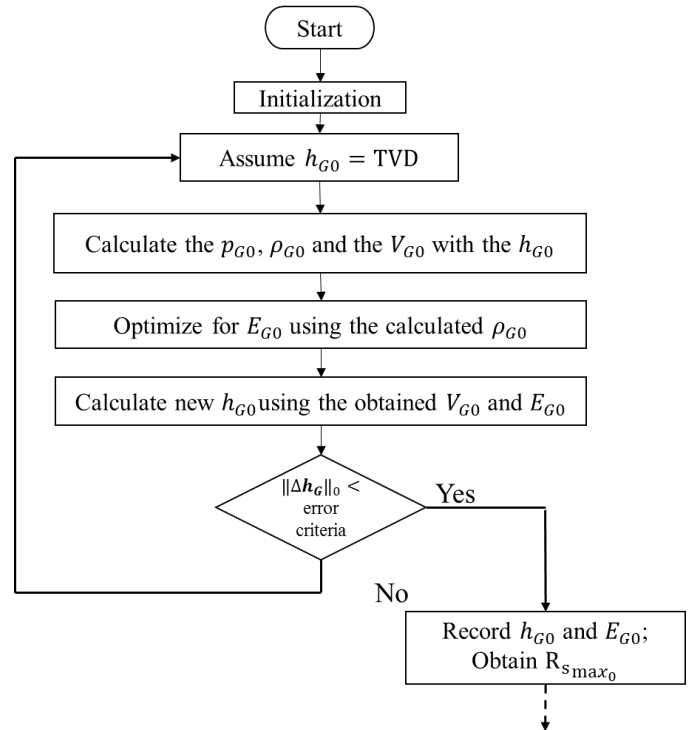


Figure 2: Obtaining initial values

Thus, in NAM, the tail of the contaminated section migrates at a velocity calculated from (9) and the volume is obtained from (6). It is important to note however that the mass at the end of a time step will not be the same as that at the end of the previous time step due to desorption and pressure decrease that would have occurred during the current time step. As a result, we will have a new volume that is used together with the space step to obtain a new void fraction.

Before desorption, the volume of liquid containing some dissolved gas is determined thus

$$V_L = \Delta h_G A (1 - E_G) \quad (22)$$

Then a new  $R_s$  is obtained from (19) and the new gas volume is obtained. For example, during the second time-step, the new volume is obtained thus,

$$V_{G1new} = V_{G1old} + V_{L1} \Delta R_{S1} B_{G1} \quad (23)$$

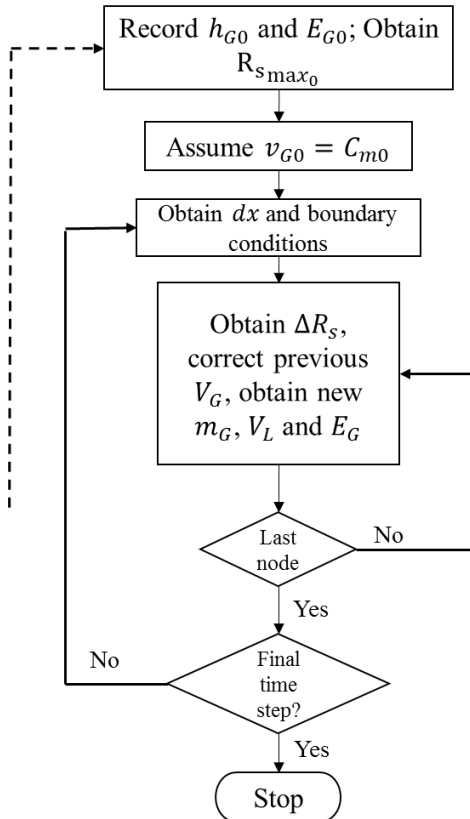


Figure 3: Algorithm flowchart for time dependent desorption of riser gas

## Results and Discussion

Diesel is assumed as the drilling fluid containing both free and dissolved gas. This has just entered the riser and is on top of the BOP. We assume an initial mass of free gas to be 150 kg and we iterate using the flow in Fig. 2. The riser length is assumed to be 1500m. An initial gas rate of  $0.004 \text{ m}^3/\text{s}$  is assumed to enable us to obtain an initial void fraction from equation. A circulation rate of  $0.006 \text{ m}^3/\text{s}$  is assumed through the booster line. An annular geometry of OD = 495. mm; ID = 127mm is assumed and a constant temperature gradient of  $20.4 - 0.025\Delta D \text{ }^\circ\text{C}$  is assumed along the riser length. The gas is reservoir gas with a specific gravity of 0.65. An interfacial tension of  $0.5\text{m}^2$  is assumed between the two phases. Mud

properties are  $9 \text{ lbm}/\text{gal}$ ; plastic viscosity of  $49 \text{ cp}$  and a yield point of  $10 \text{ lbf}/100\text{ft}^2$ . The time step remains 1s and the number of boxes remain 1000 for all cases to eliminate the effect of numerical dissipation. In this, only the contaminated mud is discretized spatially. The riser is assumed to be open to atmosphere.

### Desorption as a Time-dependent Process

This work has considered the breaking out of free gas from solution as a process that does not happen instantaneously but based on a rate as expressed by (18). For instances where we do not vary the value of the desorption coefficient in this work,  $K_d$  is assumed as  $2e^{-4}\text{s}^{-1}$ .

Figs. 4 through 6 show the behavior of influx being circulated out of riser under a time dependent desorption assumption. From Fig. 4, the sharp change in the curve path is observed at the riser equilibrium point. This occurs at a depth of 600m, 11 minutes after circulation has begun. The influx mud mixture is circulated out at  $90\text{gal}/\text{min}$  and Fig. 4 shows a continuous increase in the length of contaminated mud section. Rapid unloading has just begun, and the top of the gas section is expanding rapidly to the surface.

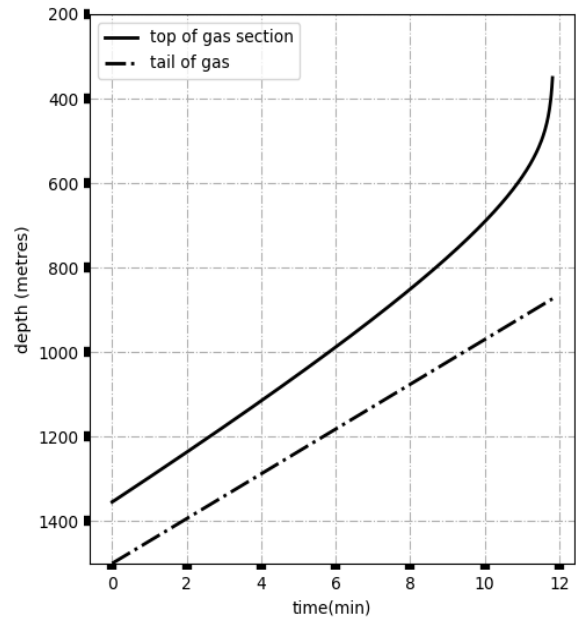
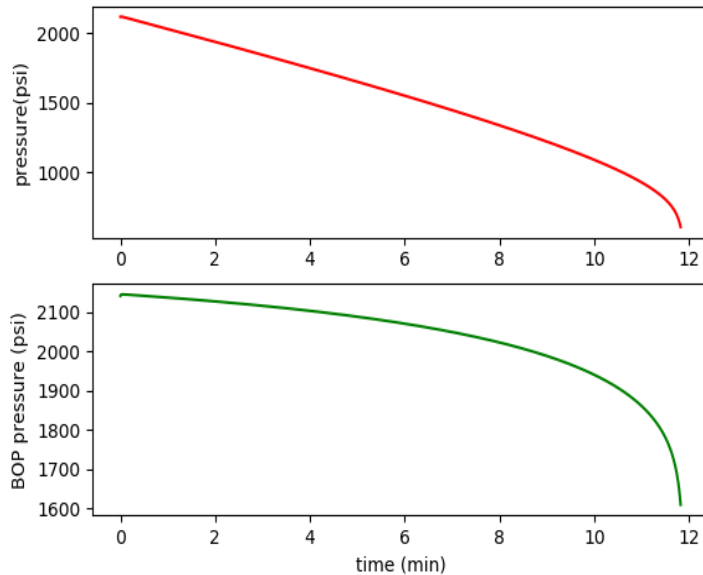


Figure 4: Position of the top and tail of the gas contaminated section in NAM assuming a time-dependent mass transfer. ( $\Delta x = h/1000$ ;  $\Delta t = 1\text{s}$ ). The sharp change in the direction of the curve path is seen as the riser equilibrium point.

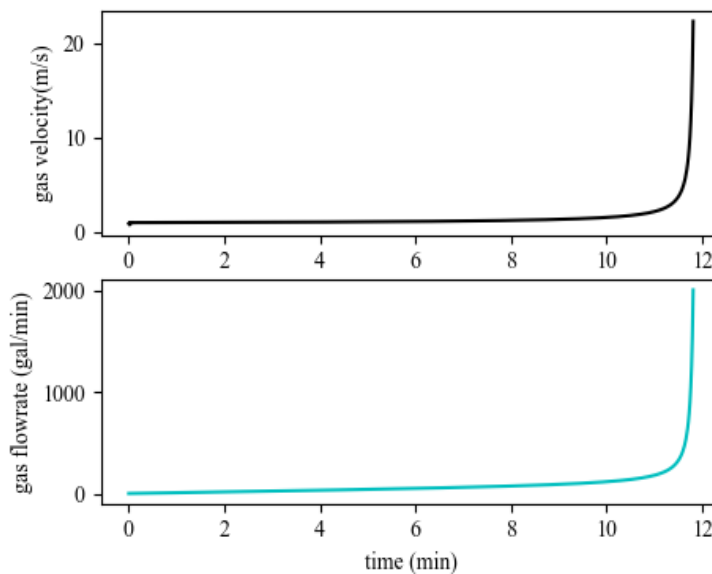
From Fig. 5, we observe the sharp change in the pressure on top of the gas section and the time this change begins as around 11 minutes with a gas pressure of about 800psi. The pressure at the BOP is shown below and a non-linear drop in pressure is observed from the start of circulation. This plot however does not clearly indicate the time rapid unloading initiates.

Fig. 6 depicts the change in top of gas velocities and top of gas flowrate as circulation progresses. The top of gas flowrate

is a function of the void fraction. The time rapid unloading initiates is also represented in the figure as around 11 minutes. The velocities attained by the expanding gas will be very high as calculated by the simulator and may not be possible in real life. From the figure the top of the gas attains a velocity of  $> 20$  m/s after the riser equilibrium point has been met by the top of the gas section.



**Figure 5:** Pressure on top of the gas section (top plot) and pressure at the BOP (bottom plot) in NAMs assuming a time-dependent mass transfer. ( $\Delta x = h/1000$ ;  $\Delta t = 1s$ ). The riser equilibrium point is not represented in the BOP pressure plot.



**Figure 6:** Gas velocities (top plot) and gas flow rates (bottom plot) until after riser equilibrium in NAMs assuming a time-dependent mass transfer. ( $\Delta x = h/1000$ ;  $\Delta t = 1s$ ).

**Figs. 7 through 9** compare results of the behavior of influx

being circulated out of riser under a time dependent desorption assumption and instantaneous desorption assumption. Rapid unloading initiates earlier and slightly deeper when we assume that degassing occurs instantaneously.

When an instantaneous assumption is assumed, the riser equilibrium point is observed as 550m depth with rapid unloading beginning after 8 minutes of circulation. When a time dependent desorption is assumed, unloading begins after 11 minutes as already indicated by **Fig 5.**, the riser equilibrium point exists at 600m.

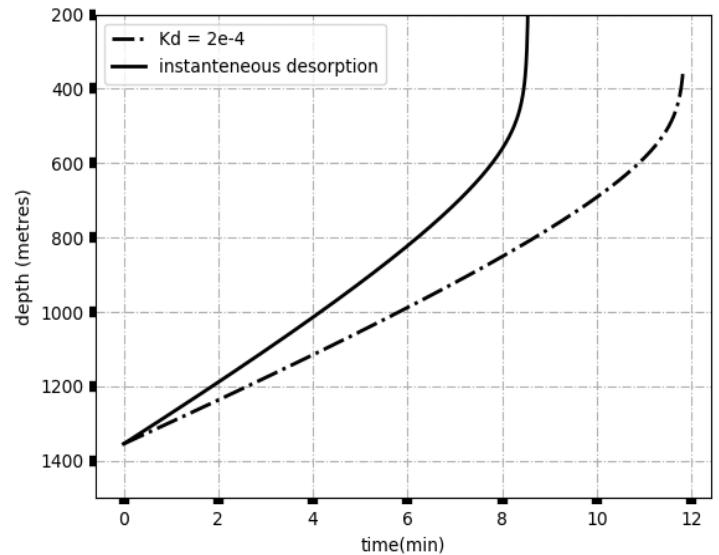


**Figure 7:** Comparison of position of the top of the gas contaminated section in NAM assuming a time-dependent and instantaneous mass transfer. ( $\Delta x = h/1000$ ;  $\Delta t = 1s$ ).

In **Fig. 8** the difference in the paths of the pressure on top of gas and the pressure at the BOP are both observed. At an instant, the pressure drop for the case of instantaneous desorption is seen to be more than the case of a time dependent desorption process. An explanation for this would be retainment of gas in the liquid as specified by the assumption of using a kinetic sub-model.

The time rapid unloading begins under both assumptions is also seen in **Fig. 9**. The figure shows a maximum attainable velocity for the top of gas as  $> 100$ m/s under an instantaneous degassing assumption. The figure does not show the maximum attainable velocity for top of gas under a time-dependent degassing assumption. This will be seen in **Fig. 11**. The flowrate of top of gas, determined as a function of void fraction, is also shown in **Fig. 9**. Like the velocities, the maximum attainable is not shown for a case of time-dependent mass transfer.

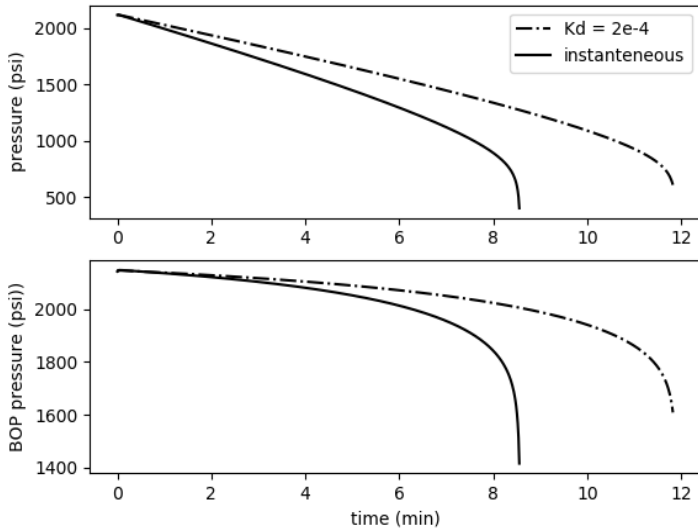


Figure 8: Comparison of pressure on top of the gas section (top plot) and pressure at the BOP (bottom plot) in NAMs under the assumption of a time-dependent mass transfer and under an assumption of instantaneous mass transfer. ( $\Delta x = h/1000; \Delta t = 1s$ ).

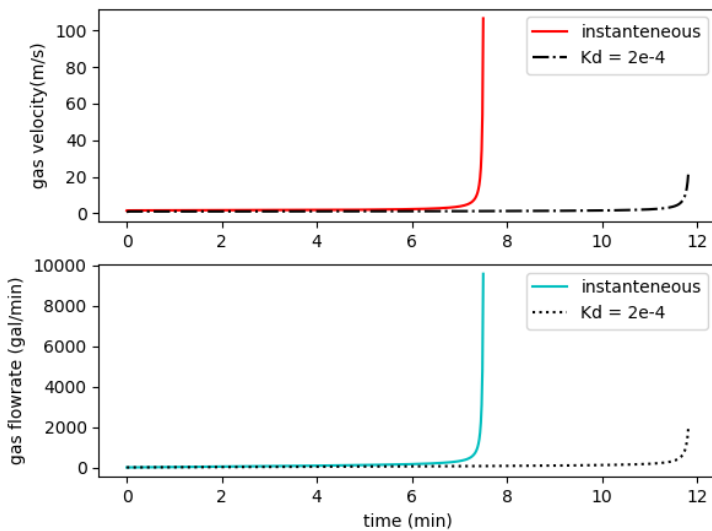


Figure 9: Comparison of gas velocities (top plot) and gas flow rates (bottom plot) until after riser equilibrium in NAMs under the assumption of a time-dependent mass transfer and under an assumption of instantaneous mass transfer. ( $\Delta x = h/1000; \Delta t = 1s$ ).

**Effect of Desorption Coefficient**

A sensitivity of simulation results to the value of desorption coefficient is examined. Although it is stated in the literature<sup>4,12</sup> that  $K_d$  depends on the fluid types and flow characteristics, there is very little information in the literature about the value of  $K_d$  that should be used for diesel-reservoir gas combination. The values of  $K_d$  used for the sensitivity analysis are obtained from the Bjørkevoll et al.<sup>12</sup> work. The degassing rates used in

this analysis include  $[2e^{-4}, 2e^{-3}, 2e^{-2}, 2e^{-1}, 2]s^{-1}$ . Interestingly, the curves all fall between the curves for an instantaneous case and no mass-transfer (WBM) case. Determination of  $K_d$  will be experimental<sup>4,12</sup>.

Fig. 10 explores the change in the position of the top of gas as a function of both time and desorption coefficient. The depth of riser equilibrium decreases with the assumed specific rate of degassing. The time rapid unloading initiates, on the other hand, increases as desorption coefficient reduces.

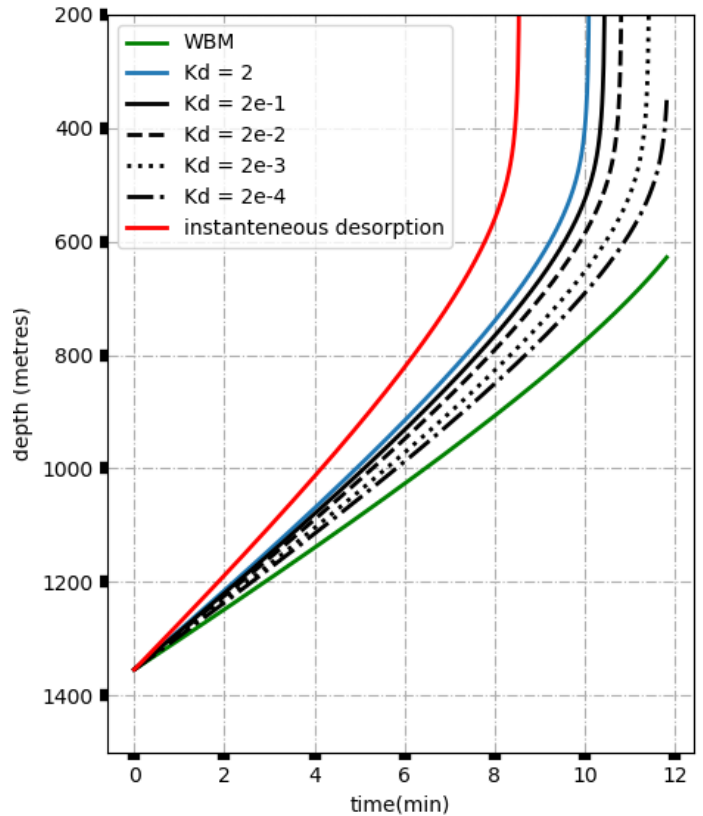


Figure 10: Effect of desorption coefficient on position of top of gas contaminated section with time. ( $\Delta x = h/1000; \Delta t = 1s$ ).

Fig. 11 depicts the pressures on top of gas and at BOP as functions of both the desorption coefficient and time. As observed, the time rapid unloading initiates is observed in the pressure on top of gas plot. As the degassing coefficient reduces, rapid unloading initiates later. The pressure the gas has at riser equilibrium point increases very slightly with reduced desorption coefficient.

Fig. 12 shows both the top of gas velocities and flowrates as functions of time and desorption coefficient. A normal trend is a reduction in the maximum velocities and flowrate with desorption coefficient. But an anomaly is seen when  $K_d = 2e^{-1}$ .

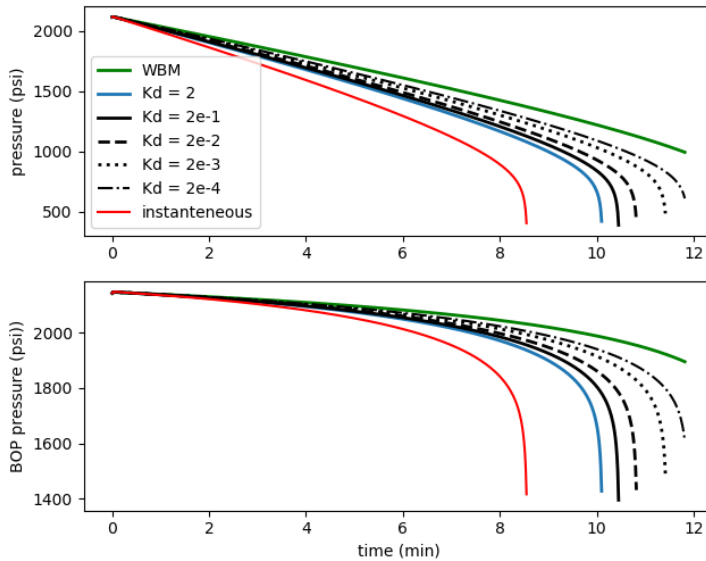


Figure 11: Effect of desorption coefficient on pressure on top of the gas section (top plot) and pressure at the BOP (bottom plot) in NAMs. ( $\Delta x = h/1000; \Delta t = 1s$ ).

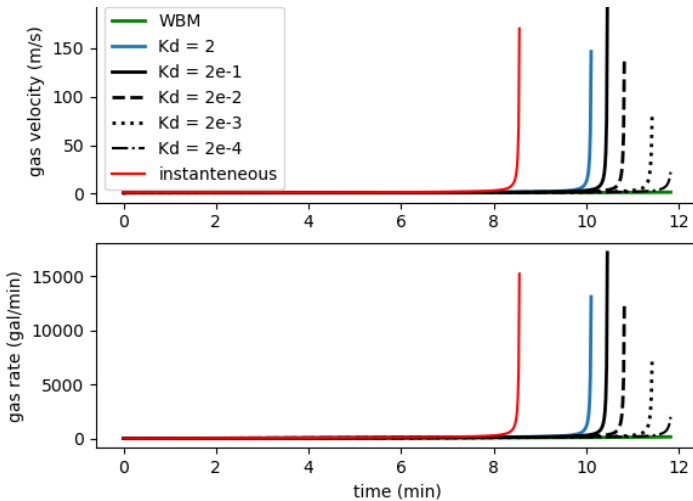


Figure 12: Effect of desorption coefficient on gas velocities (top plot) and gas flow rates (bottom plot) until after riser equilibrium in NAMs. ( $\Delta x = h/1000; \Delta t = 1s$ ).

### Drift Flux Model versus New Simplified Model

The simplicity of the drift-flux model is beneficial in many petroleum engineering applications<sup>13</sup>. Thus, for many kick simulations, the drift flux model is used.

The drift flux model can also be used for gas in riser events although with more computational difficulty and time than the simplified model proposed in this paper. The drift flux model comprises of three differential equations and several closure equations including the desorption sub-model. Solving the

model involves solving the system of differential equations simultaneously using a numerical method. The model therefore discretizes the entire pipe length initially using constant time and space step throughout the entire simulation.

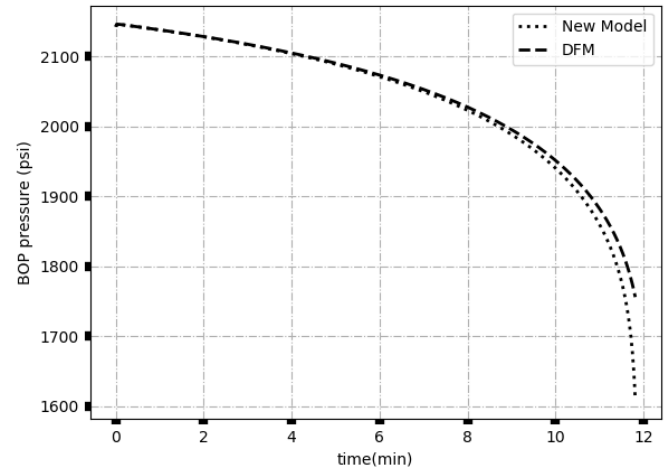


Figure 13: BOP pressure for drift flux model vs New model. ( $\Delta x = h/1000; \Delta t = 1s$ ).

This newly proposed model, on the other hand, tracks the bottom and top of the contaminated mud section, discretizes using prescribed number of boxes and obtains the values of fluid properties from the equations stated in the methodology. The drift flux model renders more accuracy as seen in **Figs. 13 and 14** because it is more rigorous. However, the difference in results is marginal and this new simplified model can serve to be a qualitative representation of gas in riser event without being too far off from accuracy.

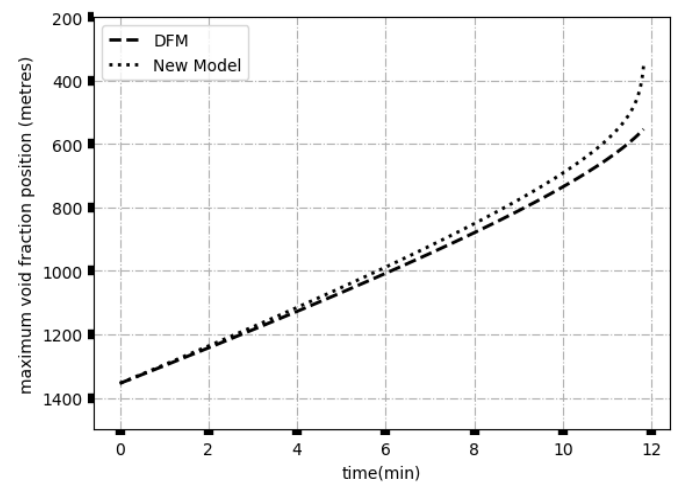


Figure 14: Position of maximum void fraction for drift flux model vs New model. ( $\Delta x = h/1000; \Delta t = 1s$ ).

## Conclusions

A simplified model has been formulated for gas in riser simulations in NAMs factoring-in degassing as a time dependent process. The time-dependent kinetic sub-model by Linga et al.<sup>4</sup> is used to quantify the desorption process.

A time-dependent desorption assumption reduces the severity of the predicted results from when an instantaneous desorption is assumed. The riser equilibrium point is shallower and unloading occurs later when a time-dependent consideration is made. Because of the shallower riser equilibrium in the time-dependent consideration, the pressure on top of the gas section is lower. When a choke backpressure is applied, less pressure will be required in simulations to maintain the same control that would be maintained in an instantaneous case desorption.

Because the mass transfer coefficient has not been established, a sensitivity analysis is conducted to see the effect of coefficient change on results. The results are very sensitive to very minor changes in mass transfer coefficient. The severity of unloading increases tremendously with small increments in the mass transfer coefficients although minor changes are seen in the riser equilibrium point. Since a mass transfer coefficient (which is at least dependent on the compositional similarity of the two phases) is not yet established, conservatively, an instantaneous desorption is assumed practically. Future laboratory tests aim to determine mass transfer coefficients for different two-phase mixtures.

This model can predict gas in riser events where degassing occurs with acceptable accuracy.

## Acknowledgments

The authors would like to thank the financial supports from National Academy of Science Gulf Research Program, and Louisiana State University Craft & Hawkins Department of Petroleum Engineering.

## Nomenclature

$p$	Pressure [Pa, psi]
$T$	Temperature [°C]
$v$	Velocity [m/s]
$\mu$	Viscosity [cp]
$V$	Volume [m <sup>3</sup> ]
$D$	Diameter [m]
$g$	Acceleration due to gravity [m/s <sup>2</sup> ]
$m$	Mass [kg]
$E$	Hold up
$Q_0$	Circulation rate [m <sup>3</sup> /s]
$\rho$	Density [kg/m <sup>3</sup> ]
$f$	Friction factor
$Re$	Reynold's number
$C_0$	Distribution parameter
$C_m$	Velocity of tail of bubble [m/s]
$h_G$	Position of top of bubble [m]
$h_m$	Position of tail of bubble [m]

$K_d$	Time-dependent desorption coefficient [s <sup>-1</sup> ]
$A$	Cross-sectional area [m <sup>2</sup> ]
$\theta$	Riser inclination [°]
$R_s$	Solubility ratio [m <sup>3</sup> /m <sup>3</sup> ]
$B$	Formation volume factor [m <sup>3</sup> /m <sup>3</sup> ]
$\sigma$	Surface tension [m <sup>2</sup> ]
EOS	Equation of state
$M_g$	Gas molecular mass

## Subscripts

$G$	Gas
$L$	Liquid
$SG$	Superficial Gas
$SL$	Superficial Liquid
$M$	Mixture
$o$	Outer
$i$	Inner
$Gr$	Drift
$max$	Maximum
$c$	Choke
$tp$	Two-phase
$0$	Initial

## References

- Caetano, E.F. (1986). *Upward Vertical Two-Phase Flow through an Annulus (Pattern, Gradient, Friction)*. The University of Tulsa, Ann Arbor, p. 242, 242 p.
- Gomes, D., Nilsen, M.S., Frøyen J., Bjørkevold, K.S., Lage, A.C.V.M., Fjelde, K.K. & Sui, D. (2018). *A Transient Flow Model for Investigating Parameters Affecting Kick Behavior in OBM for HPHT Wells and Backpressure MPD systems*. ASME paper 77547 presented at the 2018 ASME 37th International Conference on Ocean, Offshore and Arctic Engineering OMAE2018 June 17 - 22, 2018, Madrid, Spain.
- Hibiki, T., Ishii, M. (2003). *One-dimensional drift-flux model and constitutive equations for relative motion between phases in various two-phase flow regimes*. Int. J. Heat Mass Transf. 46, 4935e4948.
- Linga, H., Nilsen, F. P. & Knudsen, B.P., (2003). *Prediction Model Optimises H2S Scavenger Injection Strategy*. Sulphur 2003, 1-16. Banff, Canada.
- O'Bryan, P.L. (1988). *An Experimental Study of Gas Solubility in Oil-Based Drilling Fluids*. SPEDE (March 1988) 33–42.
- Redlich, O. & Kwong, J.N.S. (1949). *On the Thermodynamics of Solutions—V. An Equation of State. Fugacities of Gaseous Solutions*. Chemical Reviews (1949) 44, 233–244.
- Yuan, Z., Morrell, D., Sonnemann, P. & Leach, C. (2017). *Mitigating Gas-in-Riser Rapid Unloading for Deepwater-Well Control*. June 2017, SPE Drilling & Completion, pp 105-111
- Zuber, N. & Findlay, J.A. (1965). *Average volumetric concentration in two-phase flow systems*. J. Heat Transf. 87, 453e468
- Velmurugan, N., Godhavn, J.-M., & Hauge, E. (2016). *Dynamic Simulation of Gas Migration in Marine Risers*.

- SPE paper 180022-MS presented at the 2016 Bergen One Day Seminar held in Bergen, Norway, 20 April. doi:10.2118/180022-MS
10. Udegbumam, J.E., Fjelde, K.K. & Sui, D. (2018). *Numerical Integration of the AUSMV Scheme with a Dynamic Wellbore Temperature Model*. ASME paper 77493 presented at the 2018 ASME 37th International Conference on Ocean, Offshore and Arctic Engineering OMAE2018 June 17 - 22, 2018, Madrid, Spain.
  11. Xu, Z., Song, X., Li, G., Kan, W., Pang, Z. & Zhu, Z. (2018). *Development of a transient non-isothermal two-phase flow model for gas kick simulation in HTHP deep well drilling*. Applied Thermal Engineering 141 (2018) 1055–1069.
  12. Bjørkevoll, K. S., Skogestad, J. O., Frøyen, J., & Linga, H. (2018). *Well Control Simulator: Enhancing Models with Compositional PVT Models and Kinetics*. Presented at the IADC/SPE Drilling Conference and Exhibition held in Fort Worth, Texas, 6–8 March. IADC/SPE-189651-MS. doi:10.2118/189651-MS
  13. Zhou Y., Wojtanowicz A. K., Li X., Miao Y. & Chen Y. (2018). *Improved model for gas migration velocity of stagnant non-Newtonian fluids in annulus*. Journ. Of Petroleum Science and Engineering 168(2018) 190-200
  14. Lee A.L., Gonzalez M.H. & Eakin B.E. (1966) *The viscosity of natural gases*, J. Petrol. Technol. 18 (1966) 997–1000.